Astronomy & Astrophysics manuscript no. slimbh_mass_of_HLX1
March 26, 2014
©ESO 2014

arXiv:1403.6407v1 [astro-ph.HE] 25 Mar 2014

Investigating the mass of the intermediate mass black hole candidate HLX-1 with the `slimbh` model

Odele Straub[1] ⋆, Olivier Godet[2,3], Natalie Webb[2,3], Mathieu Servillat[4,1], and Didier Barret[2,3]

[1] Laboratoire Univers et Théories, CNRS UMR 8102, Observatoire de Paris, Université Paris Diderot, 5 Place Jules Janssen, F-92195 Meudon, France.
[2] Institut de Recherche en Astrophysique and Planétologie (IRAP), Université de Toulouse, UPS, 9 Avenue du colonel Roche, F-31028 Toulouse Cedex 4, France
[3] CNRS, UMR5277, F-31028 Toulouse, France
[4] Laboratoire AIM, CEA Saclay, Bat. 709, F-91191 Gif-sur-Yvette, France

Draft version

ABSTRACT

In this paper we present a comprehensive study of the mass of the intermediate mass black hole candidate HLX-1 in the galaxy ESO 243-49. We analyse the continuum X-ray spectra collected by *Swift*, *XMM-Newton*, and *Chandra* with the slim disc model, `slimbh`, and estimate the black hole mass for the full range of inclination (inc = 0° − 85°) and spin ($a_* = 0 - 0.998$). The relativistic `slimbh` model is particularly suited to study high luminosity disc spectra as it incorporates the effects of advection, such as the shift of the inner disc edge towards smaller radii and the increasing height of the disc photosphere (including relativistic ray-tracing from its proper location rather than the mid-plane of the disc). We find for increasing values of inclination that a zero spin black hole has a mass range of 6,300 - 50,900 $M_\odot$ and a maximally spinning black hole has a mass between 16,900 - 191,700 $M_\odot$. This is consistent with previous estimates and reinforces the idea that HLX-1 contains an intermediate mass black hole.

Key words. accretion, accretion discs – X-rays: binaries, black hole.

1. Introduction

There is a limit to how luminous an object of a given mass can be. When a star or an accretion disc is in hydrostatic equilibrium it supports itself against gravity by its own internal radiation pressure. The critical luminosity (assuming isotropic emission) is thus given by the Eddington limit, $L_{\rm Edd} = 4\pi c GMm_{\rm p}/\sigma_{\rm T} = 1.26 \times 10^{38}\,(M/M_\odot)$ erg/s, where c is the speed of light, G is the gravitational constant, M is the mass of the gravitating body, $m_{\rm p}$ and $M_\odot$ are the proton and solar mass, respectively, and $\sigma_{\rm T}$ is the Thompson cross-section. There are, however, objects whose luminosities exceed this natural limit.

Ultraluminous X-ray sources (ULXs) are sources with X-ray luminosities $\gtrsim 10^{39}$ erg/s. The majority of ULXs are thought to be powered by super-Eddington accretion onto a stellar mass black hole which can be accomplished (i) by powering strong disc winds (Shakura & Sunyaev 1973; Lipunova 1999), (ii) by advecting the radiation along with the flow as in radiation pressure dominated disc models like Polish doughnuts (Abramowicz et al. 1978; Jaroszynski et al. 1980) and slim discs (Abramowicz et al. 1988), or (iii) both, advection and outflows (Poutanen et al. 2007; Dotan & Shaviv 2011). Luminosities up to 10^{41} erg/s can therefore still be explained by super-Eddington mass accretion rates onto stellar mass black holes which can have maximum masses up to $\sim 80\,M_\odot$. These higher mass black holes can be explained by direct collapse of (metal poor) stars (Belczynski et al. 2010).

The brightest known ULX in the sky is 2XMM J011028.1-460421 in the lenticular galaxy ESO 243-49 (z = 0.0223, Wiersema et al. 2010). With peak luminosities $\sim 10^{42}$ erg/s this object, dubbed HLX-1 (Farrell et al. 2009), belongs to a subclass of ULXs called the hyper luminous X-ray sources (HLX, Gao et al. 2003). Like many X-ray binaries, HLX-1 shows transitions from low/hard to high/soft states (Godet et al. 2009; Servillat et al. 2011), transient radio emission that can be associated with hard-to-soft transitions (Webb et al. 2012) and a weak optical counterpart (Soria et al. 2010). The extremely high luminosity of HLX-1 suggests, however, the presence of an intermediate mass black hole (IMBH) with a mass of about $100M_\odot$ to $\sim 10^5 M_\odot$.

HLX-1 spectra have already been studied with various disc models. These were either limited to one particular inclination and/or black hole spin, non- or semi-relativistic, or based on the standard Shakura & Sunyaev (1973) disc and therefore only valid in the lowest luminosity regime, $L \lesssim 0.1 L_{\rm Edd}$. All previously used models agree that HLX-1 contains an IMBH. Servillat et al. (2011) predict a black hole mass $M > 9000 M_\odot$ from fitting the non-relativistic `diskbb` model to multi-epoch data collected by *Swift*, *XMM-Newton* and *Chandra*. Davis et al. (2011) improve the mass constraints using a relativistic thin disc model with full radiative transfer, `bhspec`, and find $3000M_\odot < M < 3 \times 10^5 M_\odot$. They assume a mass range of $1778 - 316228 M_\odot$, consider spins $a_* = -1 - 0.99$ and luminosities between $0.03 - 1 L_{\rm Edd}$ and fit simultaneously for the degenerate mass and spin parameters. As a consequence, a large fraction of their fits peg at the boundary value of at least one of these free parameters, and the results from different spectra are inconsistent with each other. In addition, the majority of their fits require luminosities far higher than the standard disc models allows. Godet et al. (2012) address the latter point by employing a simplified slim disc model that includes Comp-

⋆ E-mail: odele.straub@obspm.fr (OS)

Table 1. Observational data

Obs. Name	Instrument	Obs. ID	Start Date	End Date
Swift	*Swift* - XRT	00031287(001-252)	2008-10-24	2012-09-16
		00032577(001-011)	2012-10-02	2012-11-11
XMM-Newton	*XMM* - EPN	0560180901	2008-11-28	2008-11-28
Chandra	*Chandra* - ACIS	13122	2010-09-06	2010-09-07

tonization and some relativistic corrections (Kawaguchi 2003) and estimate $M \sim 2 \times 10^4 M_\odot$. They fit for a large mass range between $1 - 10^5 M_\odot$ and have a disc structure that allows for high luminosities, but their study is limited to a face-on disc around a Schwarzschild black hole.

In this work we are resolving the previous shortcomings regarding parameter space, luminosity regime and consistency among results from different spectra. We use a *fully* relativistic slim disc model (Sądowski et al. 2011; Straub et al. 2011) that accounts on the one hand for effects related to high mass accretion rates such as advection of radiation, relocation of the inner disc edge towards radii smaller than the innermost stable circular orbit (ISCO) and extended disc height. On the other hand, the model incorporates full vertical radiative transfer by integrating the emission of local annuli spectra and ray-tracing from the proper photosphere location. This slim disc model, `slimbh`, is valid for luminosities up to 1.25 $L_{\rm Edd}$ and covers all inclinations and (prograde) spins. It differs from the well known disc model `bhspec`, which is based on a standard thin disc, only in the structure of the underlying disc (the spectral differences between these two models have been studied in Straub et al. 2013, e.g., their Section 3.2 and the top panel in their Fig.4). In comparison to the Kawaguchi (2003) slim disc, `slimbh` is fully relativistic and uses full radiative transfer.

We are presenting results from fitting three thermal X-ray spectra of HLX-1 taken by *Swift*, *XMM-Newton* and *Chandra*. With the employed slim disc model we are not only able to study the whole parameter plane spanned by black hole spin and inclination we also get a consistent mass estimation for all spectra. This improves and solidifies the previous mass estimates. The paper contains a brief summary about the data selection in Section 2, a discussion about spectral fitting with the slim disc model in Section 3 and a summary of the results in Section 4. We finish with conclusions in Section 5

2. X-ray data reduction

We consider the three spectra listed in Table1. The *XMM-Newton* and *Chandra* spectra are the same as those studied in Servillat et al. (2011) and Godet et al. (2012). To enhance the visibility of a possible high energy tail the *Swift* spectrum consists of an accumulation of $\sim$ 121 ks of Photon Counting data near the outburst peak between 2009 and 2012 (the plateau phase – see Godet et al. 2012). The *Swift*-XRT Photon Counting data (ObsID 31287 & 32577) were processed using the HEASOFT v6.14, the tool XRTPIPELINE v0.12.8 [1] and the calibration files (CALDB version 4.1). We used the grade 0-12 events, giving slightly higher effective area at higher energies than the grade 0 events, and a 20 pixel (47.2 arcseconds) radius circle to extract the source and background spectra using XSELECT v2.4c. The background extraction region was chosen to be close to the source extraction region and in a region where we are sure that there are no sources present in the *XMM-Newton* field of view. The ancillary response files were created using XRTMKARF v0.6.0 and exposure maps generated by XRTEXPOMAP v0.2.7. We fit the spectrum using the response file SWXPC0TO12S6_20010101v012.RMF. Each spectrum was grouped to contain a minimum of 20 counts per bin to optimise the χ^2-technique.

3. Modelling the thermal spectra of HLX-1

The spectral model `slimbh` (after Abramowicz et al. 1988; Sądowski et al. 2011) is an additive disc model to be used in XSPEC (Arnaud 1996) and publicly available[2]. Like `bhspec`, this is a relativistic α-disc model with full radiative transfer - but instead of using the standard thin disc it is based on a *slim* disc, i.e., it incorporates the effects of advection. This means that with rising mass accretion rate an increasing fraction of photons gets trapped in the flow, carried inward and is partly released at smaller radii. A typical `slimbh` disc is therefore softer below the spectral peak and harder above it in comparison to `bhspec`.

The `slimbh` model has nine parameters: Black hole mass M, black hole spin a_*, disc luminosity L_{disc}, inclination i, viscosity α, distance D, hardening factor f_{hard}, limb darkening $lflag$ and vertical extent $vflag$. The latter two are flags to switch on/off the effect of limb darkening and ray-tracing from the proper disc photosphere (both are switched on here). The hardening factor is calculated internally based on the TLUSTY grid of local annuli spectra (Hubeny & Lanz 1995) which are then integrated over the whole disc (alternatively, f_{hard} could also be set to a constant colour correction factor). Using the cosmological parameters from the WMAP5 results (H_0 = 71 km s^{-1} Mpc^{-1}, Ω_M = 0.27 & Ω_Λ = 0.73), we adopt a source distance of D = 95 Mpc. The viscosity parameter is fixed at α = 0.01 which is a typical value for X-ray binary sources. A discussion of how higher values of α affect the spectra can be found in Section 4.2 and in Straub et al. (2011, 2013). The inclination is fixed at values between the model limits $0° - 85°$ in steps of $10°$. The disc luminosity is left free to assume the best fit value within the model limits $L_{disc} = 0.05 - 1.25 L_{\rm Edd}$. Our current upper inclination and luminosity limits are defined by the range of the TLUSTY grid and the internal calculation of the hardening factor from it. Like in the `bhspec` and `kerrbb` models the black hole mass and spin are degenerate parameters and cannot be fitted at the same time. When both parameters are left free, the joint confidence contours for M and a_* tend to reveal either chains of local minima, a completely unconstrained a_*, or the pegging of the spin and/or luminosity parameter at a boundary value (see Davis et al. 2011). To perform better fits and avoid such inconclusive results either the mass or spin parameter must be fixed. We freeze the spin at values between $a_* = 0.0 - 0.998$ in steps of 0.1 and fit for the mass. This procedure leads to well constrained masses

[1] `http://heasarc.gsfc.nasa.gov/docs/swift/analysis/`

[2] `http://astro.cas.cz/slimbh`

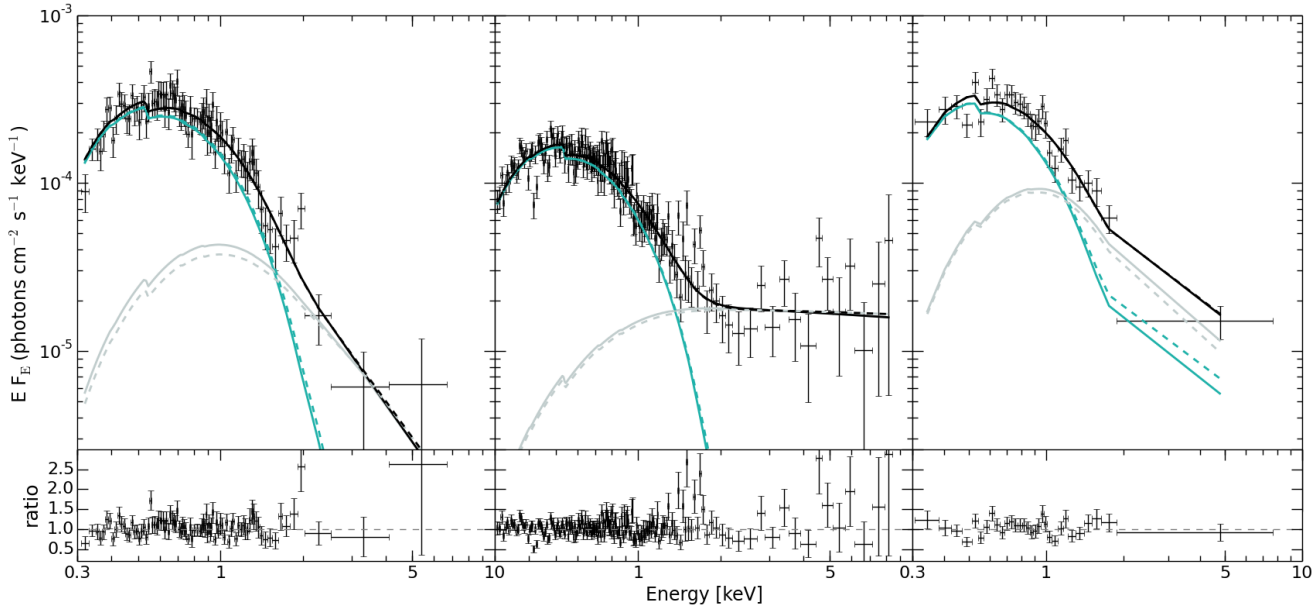

Fig. 1. *Swift* (left), *XMM-Newton* (middle) and *Chandra* (right) spectra fitted with `slimbh`. Each model consists of a disc and a Compton component (cyan and grey, respectively) and represents the best fit for the case $a_* = 0.5$, $i = 60°$ and $\alpha = 0.01$ (compare Table 2). The dashed components indicate the best fits of the same configuration when $\alpha = 0.1$.

and luminosities that are consistent among the employed data sets. All three spectra show a notable amount of statistically low significance residuals below 2 keV that might be due to narrow emission lines (see Godet et al. 2012). We do not try to fit these residuals and accept that the fit statistics for the *XMM* and *Chandra* spectra is slightly above the optimum.

The *Swift* and *XMM-Newton* data were fitted with the same model, `tbabs` × (`slimbh` + `nthc`) and the *Chandra* data were in addition multiplied by `pileup` (see Servillat et al. 2011). The absorption component, `tbabs`, is used to account for the total neutral hydrogen column density along the observer's line of sight, $N_H = 4 \times 10^{20} cm^{-2}$ (Farrell et al. 2009; Godet et al. 2012). The thermal Compton component, `nthc`, consists of the free power-law photon index Γ, the electron temperature kT_e, the seed photon temperature $kT_{bb} = 0.2$ keV (Servillat et al. 2011; Godet et al. 2012), the input type for disc-blackbody seed photons, the redshift $z = 0.0223$ (Wiersema et al. 2010) and the normalisation (free). Due to the relatively large uncertainty in the data points at the highest energies the fits are not sensitive to the electron temperature. Its precise value neither influences the fitting parameters nor the goodness of fit. We therefore fix $kT_e = 5$ keV at an arbitrary value. The `pileup` component uses a frame time of 0.83 s and has only one free (grade morphing) parameter that can assume values between 0 and 1.

4. The mass of HLX-1

We study the parameter plane spanned by black hole spin and inclination and find the distribution of black hole mass shown on the left panel in Figure 2. The shaded areas indicate the 90% confidence interval for the whole spin range. Singled out as black lines are the masses (90% confidence) we obtained for $a_* = 0.5$. The open and filled circles mark previous results (error bars have been omitted) of Davis et al. (2011) and Godet et al. (2012), respectively. The mass estimates from the *Chandra* spectrum (grey), which is affected by pileup, seem to slightly overestimate the black hole mass as compared to the *Swift* (green) and *XMM* (blue) spectra which are almost congruent. They are, however, consistent within the error bars. This behaviour does not apply to the results of Davis et al. (2011), where the highest mass at a given inclination is associated with a *Swift* or *XMM* spectrum and a spin that pegs at the maximum value. In general, higher inclinations implicate larger black hole masses as the geometrically induced reduced photon count is compensated with a higher source mass. With increasing spin the radiation originates from an ever smaller area around the black hole, which also translates into a reduced amount of photons and consequently a larger black hole mass. To show the effect of the black hole spin in detail we plot in the right panel of Figure 2 the masses for *Swift* spectrum alone. Given a Schwarzschild black hole and a face-on disc, the mass found by Godet et al. (2012) is substantially higher than the one found with models that include full radiative transfer.

The *XMM* spectrum requires a significant amount of Comptonisation to model the high energy tail (see Figure 1). The contribution of the disc to the total luminosity is thus substantially lower than for the *Swift* and *Chandra* spectrum, as shown in the left panel of Figure 3. Both, increasing spin and increasing inclination reduce the effective emission area which is efficiently compensated with increasing black hole masses during the fit procedure, while the disc luminosity does not change significantly. If, however, the configuration is set to maximal spin, the model spectrum becomes so soft below the peak that tuning the mass parameter alone is not sufficient anymore to fit the observed spectrum, instead the disc luminosity needs to be increased. This behaviour is visible in the right panel of Figure 3, where the luminosity that corresponds to the maximum spin crosses all other lines. In practice this means that in a low inclination system with uncertain black hole mass a low spin could be easily mistaken for maximally rotating black hole.

There is currently no evidence for eclipses in HLX-1, the inclination is thus likely to be lower than ca 75°. We assume here an inclination of 60° to demonstrate the modelling of the three spectra for a moderate spin, $a_* = 0.5$, in Figure 1 and the resulting parameter values in Table 2. Due to the weakness of

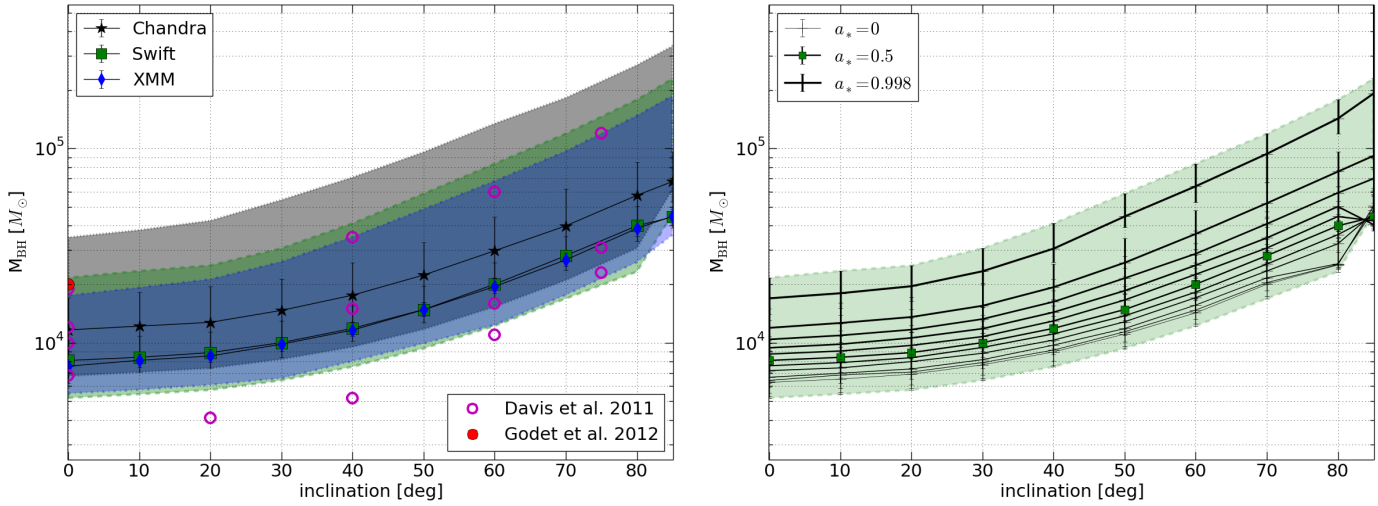

Fig. 2. The black hole mass in HLX-1. *Left*: The shaded areas indicate the 90% confidence interval for the mass estimation of the *Chandra* (grey), *Swift* (green) and *XMM* (blue) spectrum, respectively, given for the whole spin range. The three solid lines represent the black hole mass that corresponds to the spin $a_* = 0.5$ (where the error bars denote 90% confidence). The filled and open circles show previous mass measurements (see text for details). *Right*: The influence of spin on the mass estimation is shown for the *Swift* data. Error bars give the 90% confidence interval.

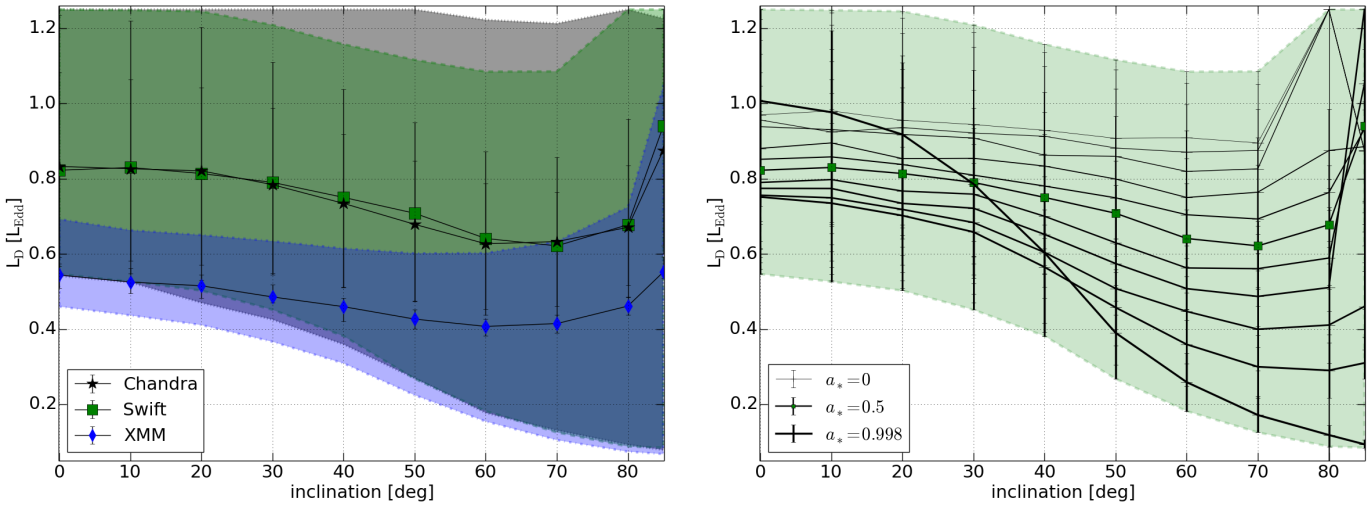

Fig. 3. The disc luminosity in HLX-1. *Left*: The shaded areas indicate the 90% confidence interval for the luminosity distribution associated with the black hole mass measured in Figure 2. Again, the the result for $a_* = 0.5$ is singled out and given by the three solid lines (with 90% confidence), corresponding, respectively, to the *Chandra* (grey), *Swift* (green) and *XMM* (blue) spectrum. *Right*: The influence of the black hole spin on the luminosity of the *Swift* spectrum. Error bars give the 90% confidence interval.

the high energy tail in the *Swift* and *Chandra* spectra the photon index, Γ, is only weakly constrained. Moreover, in the chosen example the adding of a Compton component is statistically not very significant, in particular for the *Chandra* spectrum; the F-test in XSPEC gives a probability of $p = 3 \times 10^{-18}$, $p = 0.008$ and $p = 0.178$ for the *XMM*, *Swift* and the *Chandra* data, respectively. However, as we move through the parameter space to lower black hole spins and inclinations, the Compton component becomes more significant, even for the *Swift* and *Chandra* observation. This is because for low spin and low inclination pure absorbed disc models are intrinsically too soft to properly reproduce the high energy (> 4keV) photons. As a consequence, the models with the lowest spins and inclinations, $a_* \lesssim 0.1$ and $i \lesssim 20°$, respectively, favour high disc luminosities, without Compton component they would require a luminosity higher than our current limit of $L = 1.25 L_{\rm Edd}$. Whether such models would ultimately fit the data better remains to be seen in future work.

4.1. The mass accretion rate

For a given black hole mass and spin one can deduce the accretion efficiency from $\eta = GM/R_{ms}c^2$, where R_{ms} is the spin dependent marginally stable radius that defines roughly the inner edge of the disc. The mass accretion rate is then given by $L = \eta \dot{M} c^2$ where $L = 4\pi D^2 F_{obs}$ is calculated from the unabsorbed flux in the 0.01 - 40 keV energy range. The mass accretion rate is thus proportional to the flux and decreases for increasing values of inclination and black hole spin (i.e., increasing black hole mass). We find mass accretion rates $\dot{M} \simeq 2.9{\times}10^{-5} - 1.7{\times}10^{-4}\, M_\odot\, {\rm yr}^{-1}$. These estimates are consistent with those found by (Godet et al. 2012). We note that the effective inner disc edge of the here considered slim discs lies inside R_{ms}, in particular for low spin

($a_* < 0.5$) and $L > 0.3 L_{\rm Edd}$ (see Abramowicz et al. 2010, for a discussion of the inner disc edge). While this slightly increases the efficiency, it does not significantly change the resulting mass accretion rate.

4.2. The effect of viscosity

In hydrodynamic disc models like bhspec and slimbh the relation between viscous stresses and pressure is thought to be parametrised by the viscosity parameter, α. Despite the fact that accretion discs have been studied for forty years the precise nature of this relation is still unclear and α remains a phenomenological quantity that possibly comprises of several physical mechanisms related to the pressure balance in accretion discs. We use a default value of $\alpha = 0.01$ which is supported by observations of high luminosity, radiation pressure dominated discs that require a roughly constant colour temperature correction (i.e., hardening factor) which is only supported by a low viscosity (Done & Davis 2008). We note, however, that outburst cycles in low mass X-ray binaries require a very efficient angular momentum transport and thus suggest a high α value (see, e.g., the review by Lasota 2001). We therefore perform an additional analysis assuming $\alpha = 0.1$ and find that the black hole mass increases by 7%-14%. Figure 1 shows the corresponding best fit as dashed lines. Since a larger viscosity translates into a smaller amount of thermalised photons in the plasma, which in turn entails a larger colour temperature correction, the slim disc spectra of a given luminosity get harder with increasing α. This change in the spectral shape causes a roughly 10% increase in mass. We caution, however, that a high luminosity disc becomes effectively optically thin when the viscosity is too large and therefore consider the low viscosity value as the standard (see also the discussion in Straub et al. 2011, 2013).

5. Conclusions

We analysed three spectra of the IMBH candidate HLX-1 that were collected by *Swift*, *XMM-Newton* and *Chandra* during different missions between 2008 and 2012. We estimate the black hole mass using the fully relativistic slim disc model, slimbh (Sądowski et al. 2011; Straub et al. 2011), that allows to self-consistently probe the trans-Eddington luminosity regime in the whole parameter plane spanned by black hole spin and inclination. This addresses and remedies the deficits of previously used models which were either not relativistic (Servillat et al. 2011), only valid at lowest luminosities and affected by parameter pegging (Davis et al. 2011), or only valid for one particular inclination and spin (Godet et al. 2012). Assuming a low disc viscosity ($\alpha = 0.01$) we find that a Schwarzschild black hole has a mass of about 6,300 - 50,900 $M_\odot$ (increasing with disc inclination) whereas a maximally spinning black hole has a mass between 16,900 - 191,700 $M_\odot$. A high viscosity disc ($\alpha = 0.1$) has roughly 10% higher black hole masses. This result is consistent among all three observations with *Swift*, *XMM-Newton* and *Chandra*. Moreover, it is also in good agreement with earlier measurements based on bhspec (Davis et al. 2011) and other slim disc models (Godet et al. 2012).

The here applied continuum fitting method determines the inner edge of the accretion disc given its effective temperature and flux, i.e., it is designed to measure the black hole spin and relies strongly on the knowledge of the binary parameters, M , D and i. Given that the inclination is only constrained to $i < 75°$ the constraints on the black hole mass are necessarily fairly weak. Nontheless, our results clearly place HLX-1 in the regime of intermediate-mass black holes. Future dynamical measurements of the binary parameters of HLX-1 will allow to apply the continuum fitting method as it has been intended, namely to assess the spin of the IMBH.

OS thanks the IRAP in Toulouse for their hospitality.

References

Abramowicz, M., Jaroszynski, M., & Sikora, M. 1978, A&A, 63, 221
Abramowicz, M. A., Czerny, B., Lasota, J. P., & Szuszkiewicz, E. 1988, ApJ, 332, 646
Abramowicz, M. A., Jaroszyński, M., Kato, S., et al. 2010, A&A, 521, A15
Arnaud, K. A. 1996, in Astronomical Society of the Pacific Conference Series, Vol. 101, Astronomical Data Analysis Software and Systems V, ed. G. H. Jacoby & J. Barnes, 17
Belczynski, K., Bulik, T., Fryer, C. L., et al. 2010, ApJ, 714, 1217
Davis, S. W., Narayan, R., Zhu, Y., et al. 2011, ApJ, 734, 111
Done, C. & Davis, S. W. 2008, ApJ, 683, 389
Dotan, C. & Shaviv, N. J. 2011, MNRAS, 413, 1623
Farrell, S. A., Servillat, M., Gladstone, J. C., et al. 2013, ArXiv e-prints
Farrell, S. A., Webb, N. A., Barret, D., Godet, O., & Rodrigues, J. M. 2009, Nature, 460, 73
Gao, Y., Wang, Q. D., Appleton, P. N., & Lucas, R. A. 2003, ApJ, 596, L171
Godet, O., Barret, D., Webb, N. A., Farrell, S. A., & Gehrels, N. 2009, ApJ, 705, L109
Godet, O., Plazolles, B., Kawaguchi, T., et al. 2012, ApJ, 752, 34
Hubeny, I. & Lanz, T. 1995, ApJ, 439, 875
Jaroszynski, M., Abramowicz, M. A., & Paczynski, B. 1980, Acta Astron., 30, 1
Kawaguchi, T. 2003, ApJ, 593, 69
Lasota, J.-P. 2001, New A Rev., 45, 449
Lipunova, G. V. 1999, Astronomy Letters, 25, 508
Poutanen, J., Lipunova, G., Fabrika, S., Butkevich, A. G., & Abolmasov, P. 2007, MNRAS, 377, 1187
Sądowski, A., Abramowicz, M., Bursa, M., et al. 2011, A&A, 527, A17
Servillat, M., Farrell, S. A., Lin, D., et al. 2011, ApJ, 743, 6
Shakura, N. I. & Sunyaev, R. A. 1973, A&A, 24, 337
Soria, R., Hau, G. K. T., Graham, A. W., et al. 2010, MNRAS, 405, 870
Straub, O., Bursa, M., Sądowski, A., et al. 2011, A&A, 533, A67
Straub, O., Done, C., & Middleton, M. 2013, A&A, 553, A61
Webb, N., Cseh, D., Lenc, E., et al. 2012, Science, 337, 554
Webb, N. A., Barret, D., Godet, O., et al. 2010, ApJ, 712, L107
Wiersema, K., Farrell, S. A., Webb, N. A., et al. 2010, ApJ, 721, L102

Table 2. Detailed results for *Swift*, *XMM-Newton* & *Chandra* spectra for $a_* = 0.5$ and $i = 60°$. The two error intervals for the black hole mass corresponds to the 90% and 3 σ confidence level, respectively.

Model Par.	*Swift*	*XMM-Newton*	*Chandra*
`tbabs`			
N_H [$\times 10^{20}$]		4	
`slimbh`			
M [$M_\odot$]	$19989^{+5883\ +13902}_{-3078\ -4606}$	$19387^{+1670\ +3333}_{-1436\ -2507}$	$29952^{+14476\ +36285}_{-8381\ -12201}$
a_*		0.5	
L_{disc} [$L_{\rm Edd}$]	$0.64^{+0.14}_{-0.19}$	$0.41^{+0.02}_{-0.03}$	$0.62^{+0.25}_{-0.18}$
i [deg]		60	
α		0.01	
D [Mpc]		95	
`nthc`			
Γ	$4.16^{+3.24}_{-2.57}$	$2.04^{+0.37}_{-0.29}$	$4.55^{+2.58}_{-2.50}$
kT_e [keV]		5	
kT_{bb} [keV]		0.2	
z		0.0223	
N [10^{-5}]	$4.59^{+7.27}_{-4.23}$	$1.59^{+0.55}_{-0.43}$	$11.96^{+9.12}_{-10.36}$
`pileup`			
t_{frame} [s]	-	-	0.83
f	-	-	$0.16^{+0.61}_{-0.16}$
χ^2/dof (χ^2_r)	82.07/85 (0.97)	239.77/177 (1.35)	37.84/27(1.40)